Modeling of Microwave Semiconductor Diodes

Michal POKORNÝ, Zbyněk RAIDA

Dept. of Radio Electronics, Brno University of Technology, Purkyňova 118, 612 00 Brno, Czech Republic

xpokor33@stud.feec.vutbr.cz, raida@feec.vutbr.cz

Abstract. *The paper deals with the multi-physical modeling of microwave diodes. The electrostatic, drift-diffusion and thermal phenomena are considered in the physical model of the components. The basic semiconductor equations are summarized, and modeling issues are discussed. The simulations of the Gunn Effect in transferred electron devices and the carrier injection effect in PIN diodes are investigated and discussed. The analysis was performed in COMSOL Multiphysics using the finite element method.*

Keywords

Gunn effect, carrier injection effect, PIN, FEM, COMSOL Multiphysics, drift-diffusion scheme, multi-physical model.

1. Introduction

In the 20th century, semiconductor components replaced thermionic devices (vacuum tubes) in most applications. The design and the fabrication of modern semiconductor devices involve an accurate prediction of physical parameters and behavior under specific conditions. The macro-models of a semiconductor device connect diffusion processes for the hole and electron concentration, the electric potential distribution and thermal effects. Therefore, the semiconductor device modeling represents the multi-physical problem, where strong nonlinear dependencies are present [1].

A diode belongs to the most frequently used microwave semiconductor devices. The Gunn diode is exploited for the amplification or the signal generation. A PIN diode is applied as a linear attenuator or a switching device. Thus those two devices were chosen for an investigation using a macroscopic drift-diffusion scheme.

In the paper, the SI unit system is used. Therefore, the value of certain coefficients and quantities can differ from other publications.

2. Basic Semiconductor Equations

Electrostatic and drift-diffusion equations for semiconductors can be derived from Maxwell's equations and Boltzmann transport theory. Considering various simplistic assumptions, the basic equations can be composed from Poisson's equation (1), the continuity equations for electrons (2) and holes (3), and current relations for electrons (4) and holes (5). The heat flow equation (6) allows the correct simulation of power devices [1], [2]:

$$\nabla \cdot (\nabla \psi) = \frac{q}{\varepsilon}(n - p - N) \ , \tag{1}$$

$$\nabla \cdot (\mathbf{J}_n) = qR \ , \tag{2}$$

$$\nabla \cdot (\mathbf{J}_p) = -qR \ , \tag{3}$$

$$\mathbf{J}_n = qn\mu_n \mathbf{E} + qD_n \nabla n \ , \tag{4}$$

$$\mathbf{J}_p = qp\mu_p \mathbf{E} - qD_p \nabla p \ , \tag{5}$$

$$H = -\nabla \cdot k_T \nabla T \ . \tag{6}$$

Here, ψ denotes the electrostatic potential, q is the elementary charge, ε is the permittivity, n denotes the negatively charged electron concentration, p is the positively charged hole concentration, N is the net doping concentration, $\mathbf{J}_{n,p}$ denotes the current densities caused by electrons and holes, R is the generation-recombination rate, μ represents the carrier mobility, $\mathbf{E}$ denotes the electric field vector, $D_{n,p}$ is the diffusion coefficient, H denotes the locally generated heat, k_T is the thermal conductivity and T is temperature.

The electric field vector $\mathbf{E}$ is connected with the electrostatic potential ψ by following the relation:

$$\mathbf{E} = -\nabla \psi \ . \tag{7}$$

The diffusion coefficients are defined by Einstein's relation [2]:

$$D_{n,p} = \mu_{n,p} \frac{kT}{q} \ . \tag{8}$$

Here, k is the Boltzmann constant.

3. Physical Parameters

The basic equations (1) to (8) can describe electric fields and currents in general solid media which contain free charge carriers. The proper modeling of the physical parameters can approximate the device features close to the reality.

The doping profile, which defines the geometry of the device, is given by concentrations of acceptors N_A and donors N_D. Assuming all the impurities are ionized, the fixed charge can be described by the net doping formula:

$$N = N_D - N_A \ . \tag{9}$$

The Shockley-Read-Hall recombination is the major generation-recombination process in bulk semiconductors. The process can be modeled by

$$R^{SRH} = \frac{np - n_i^2}{\tau_p \left(n + n_1\right) + \tau_n \left(p + p_1\right)} \ , \tag{10}$$

where n_i is the intrinsic carrier concentration, and τ_n and τ_p are the carrier lifetimes [1], [3]. Under specific simplifications, concentrations n_1 and p_1 can be assumed equal to n_i.

At high doping concentrations, the lifetime can be assumed to vary with doping. In [1], the following empirical expression is presented:

$$\tau_{n,p} = \frac{\tau_{n0,p0}}{1 + \dfrac{N_D + N_A}{N_{n,p}^{ref}}} \ . \tag{11}$$

The interaction with the thermally generated vibrations of the crystal lattice is the fundamental process of the carrier scattering. This effect is simply modeled by

$$\mu_{n,p}^{L} = \mu_{n,p}^{300} \left(\frac{T}{300\mathrm{K}} \right)^{-\alpha_{n,p}} \ , \tag{12}$$

where values of mobility at 300K $\mu_{n,p}{}^{300}$ and coefficients $\alpha_{n,p}$ are obtained by fitting experimental data.

	Si	GaAs
n_i	$1.25 \cdot 10^{16}$ m^{-3}	$1.45 \cdot 10^{13}$ m^{-3}
τ_p	$0{,}1 \cdot 10^{-6}$ s	$0{,}1 \cdot 10^{-6}$ s
τ_n	$0{,}1 \cdot 10^{-6}$ s	$0{,}1 \cdot 10^{-6}$ s
τ_{p0}	$3{,}52 \cdot 10^{-5}$ s	$3{,}52 \cdot 10^{-5}$ s
τ_{n0}	$3.95 \cdot 10^{-4}$ s	$3.95 \cdot 10^{-4}$ s
N^{ref}	$7.1 \cdot 10^{21}$ m^{-3}	$7.1 \cdot 10^{21}$ m^{-3}
$\mu_n{}^{300}$	0.14 m^{2}V^{-1}s^{-1}	0.8 m^{2}V^{-1}s^{-1}
$\mu_p{}^{300}$	0.04 m^{2}V^{-1}s^{-1}	0.04 m^{2}V^{-1}s^{-1}
α_n	2.2	1
α_p	2.2	2.1
k_{T300}	154.86 Wm^{-1}K^{-1}	46 Wm^{-1}K^{-1}
β	4/3	5/4

Tab. 1. Values of material quantities.

A sufficient approximation of the thermal conductivity dependence on the temperature can be modeled by

$$k_T = k_{T300} \left(\frac{T}{300\mathrm{K}} \right)^{-\beta} \ , \tag{13}$$

and the locally generated heat for a non-degenerated semiconductor is given by [1]:

$$H = \left(\mathbf{J}_n + \mathbf{J}_p\right)\mathbf{E} \ . \tag{14}$$

The values of the mentioned quantities for Si and GaAs are summarized in Table 1 [1], [2], [3], [4].

3.1 Gunn Effect

The saturation of the drift velocity of electrons in a high electric field, which corresponds to the reduction of the effective mobility, is the key parameter of the Gunn Effect. For GaAs, this effect is modeled by the combination of the following expressions [1]:

$$\mu_n^{LE} = \frac{\mu_n^L + v_{sat} \ E^3 / E_{crit}^4}{1 + \left(E / E_{crit}\right)^4} \ , \tag{15}$$

$$v_{sat} = \frac{v_{sat}^{300}}{(1 - A_n) + A_n \left(\dfrac{T}{300\mathrm{K}} \right)} \ . \tag{16}$$

Here μ_n^L represents the temperature depend mobility (12), v_{sat} is the saturation velocity, $v_{sat}{}^{300}$ denotes the saturation velocity at 300 K, E_{crit} is the threshold electric field, and A_n is the coefficient obtained by fitting experimental values of v_{sat}. The typical values for GaAs are $E_{crit} = 400 \cdot 10^3$ Vm^{-1}, $A_n = 0.56$, $v_{sat}{}^{300} = 72 \cdot 10^3$ ms^{-1} [4].

3.2 Carrier Injection Effect

As the free carrier concentrations increase, another generation-recombination mechanism becomes important. Auger recombination, also known as three-body or three-particle recombination, becomes dominant when the carrier concentration becomes very large as in the case of carrier injection in PIN diodes. A model for Auger recombination can be found in [1] and [3].

$$R^{AU} = (C_n^{AU} n + C_p^{AU} p)(np - n_i^2) \ . \tag{17}$$

The values of the Auger recombination coefficients are [1] $C_n^{AU} = 2.8 \cdot 10^{-43}$ m^{6}s^{-1} and $C_p^{AU} = 9.9 \cdot 10^{-44}$ m^{6}s^{-1}.

For the purpose of the device modeling the individual generation-recombination rates can be added up:

$$R = R^{SRH} + R^{AU} \ . \tag{18}$$

The mobility of free carriers is another important physical parameter to be considered. There are many mechanisms which cause the reduction of the carrier mobility. If the temperature dependency is ignored, the scattering caused by ionized impurities and the carrier-carrier scattering are the main mechanisms which affect carrier mobility

in PIN devices. The first one is involved due to the high doping concentration of P-type and N-type layers of the device. This effect can be modeled by [1]:

$$\mu_{n,p}^{I} = \frac{\mu_n^{300}}{\sqrt{1+\dfrac{N_D+N_A}{C_{n,p}^{ref}+\dfrac{N_D+N_A}{S_{n,p}}}}} \ . \tag{19}$$

For bulk Si the coefficients are $C_n^{ref} = 3\cdot10^{22}$, $C_p^{ref} = 4\cdot10^{22}$, $S_n = 350$ and $S_p = 81$.

The second one represents scattering by electrons and holes themselves. This is significant mechanism due to high free carrier concentrations at the intrinsic layer. The effect can be described by [1]:

$$\mu^{C} = \frac{1.04\cdot10^{23}}{\sqrt{np}\,\ln\left(1+7.45\cdot10^{17}(np)^{-1/3}\right)} \ . \tag{20}$$

In order to obtain the over all mobility, the models can be combined using the Mathiessen rule [1]:

$$\mu_{n,p}^{IC} = \frac{1}{\dfrac{1}{\mu_{n,p}^{I}}+\dfrac{1}{\mu^{C}}} \ . \tag{21}$$

4. Equations System and Boundary Conditions

In Section 2, the system of the basic equations was introduced. Substituting the current relations (4), (5) and the formula (7) into continuity equations (2) and (3), the following system of three partial differential equations (PDE) with three dependent variables Ψ, n and p is obtained [1].

$$\nabla\cdot(\nabla\psi)-\frac{q}{\varepsilon}(n-p-N)=0 \ , \tag{22}$$

$$\nabla\cdot(D_n\nabla n-n\mu_n\nabla\psi)-R=0 \ , \tag{23}$$

$$\nabla\cdot(D_p\nabla p+p\mu_p\nabla\psi)-R=0 \ , \tag{24}$$

which is the final system of PDE to be solved (using COMSOL Multiphysic in our case) in the domain of their validity. The equation (22) is the elliptic PDE and the equations (23) and (24) are parabolic PDE while the function R has no spatial derivations of the second or higher order, and the coefficients D_n, D_p, μ_n a μ_p are always positive [1].

In order to perform the numerical analysis, a priori information about the domain and the boundary conditions is needed. The enclosed domain of the analysis is three dimensional, in general. In many cases, the dimension can be reduced to decrease computational demands.

The boundary conditions can be divided into physical boundaries and artificial ones. Models presented in this paper deal with ohmic contacts (physical boundaries) and artificial boundary conditions guarantying that the domain is self-contained.

The boundary conditions for ohmic contacts are Dirichlet boundary conditions for electrostatic potential

$$\psi-\psi_b-\psi_D=0 \ , \tag{25}$$

and for carrier concentrations [1]

$$n=\frac{\sqrt{N^2+4n_i^2}+N}{2} \ , \tag{26}$$

$$p=\frac{\sqrt{N^2+4n_i^2}-N}{2} \ , \tag{27}$$

where Ψ_D denotes the applied bias voltage and Ψ_b built-in potential which can be calculated by [1]

$$\psi_b=\frac{kT}{q}\,ar\sinh\left(\frac{N}{2n_i}\right) \ . \tag{28}$$

The artificial boundary conditions which make the device self-contained are the Neumann boundary conditions for electrostatic potential

$$\frac{\partial\psi}{\partial\mathbf{n}}=0 \ , \tag{29}$$

and carrier concentrations [1]

$$\frac{\partial n}{\partial\mathbf{n}}=0 \ , \tag{30}$$

$$\frac{\partial p}{\partial\mathbf{n}}=0 \ . \tag{31}$$

5. Simulations and Results

The simulation was performed by solving the system of PDE (22-24) extended by models of relevant physical parameters (section 3).

5.1 Gunn Diode

The 2D model of a diode made of GaAs corresponds to the mesh shown in Fig. 1. The donor concentration is 10^{23} m^{-3} in the supporting layer, and 10^{21} m^{-3} in the active layer. The width of the transition between layers is 2 μm, and is of the Gaussian shape (see Fig. 2).

Fig. 3 shows the electric field distribution at the applied bias Va = 6 V. If a voltage is applied to the device, then the electric field is largest across the thin active layer, and the negative differential conductivity occurs here.

The thermal phenomenon was simulated supposing no heat sink at the cathode contact, and assuming a cooper heat sink 60 μm × 30 μm at the cathode contact. In both cases, the heat transfer coefficient was set to 5 Wm^{-2}K^{-1} at

all boundaries, which corresponds to the air as a cooling medium without convection [2]; the ambient temperature was set to 300 K (Fig. 4). Temperature distributions are practically uniform, but the surface values can reveal the center of the heat source. The arrows (vectors of heat flux) show the influence of the heat sink if the heat is significantly conducted away (see Fig. 5). The result is 21 K difference of the device temperature between both the cases. The dependence of the device temperature on the bias voltage is presented in Fig. 6.

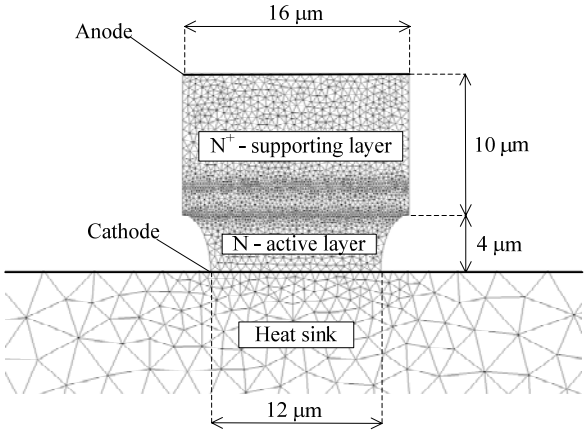

Fig. 1. Structure of Gunn diode.

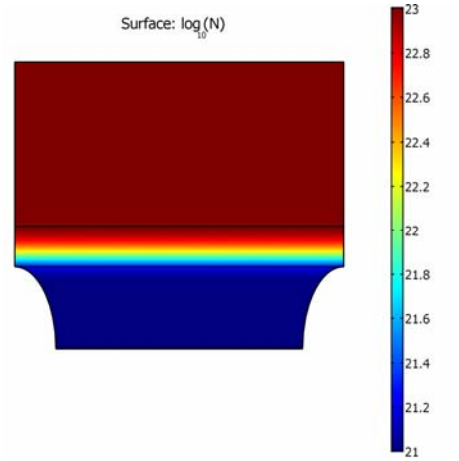

Fig. 2. Distribution of donor concentration

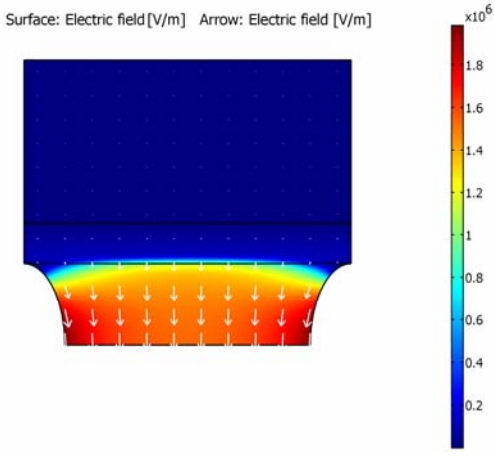

Fig. 3. Electric field distribution at applied bias $Va = 6$ V.

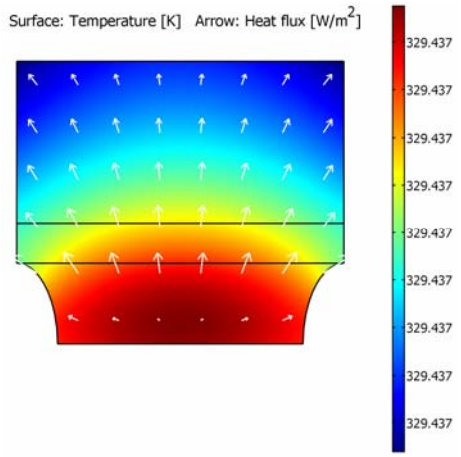

Fig. 4. Temperature distribution (surface) and heat flux (arrows) of Gunn diode at applied bias $Va = 6$ V without heat sink.

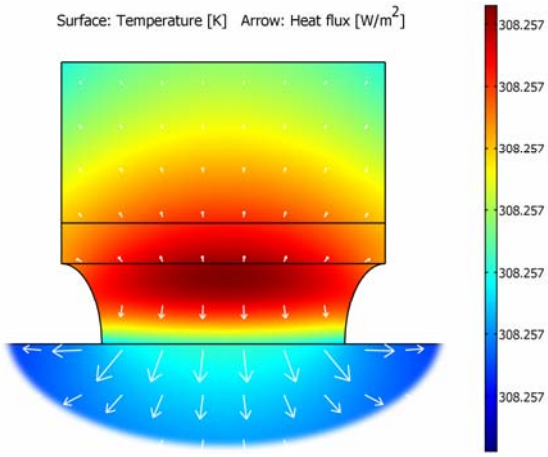

Fig. 5. Temperature distribution (surface) and heat flux (arrows) of Gunn diode at applied bias $Va = 6$ V with heat sink.

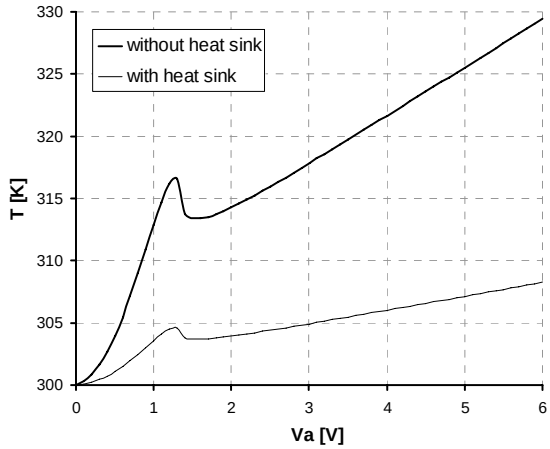

Fig. 6. T-V characteristics of Gunn diode with / without heat sink.

The I-V characteristics of the diode was obtained by the integration of the normal component of current density at the cathode boundary and moderated by a coefficient 10^{-5} m in order to obtain the proper unit of current (Fig. 7). The diode operates as a linear resistor up to the bias about $Va = 1$ V. Further increase of the bias voltage causes the decrease of the effective mobility, so the negative differen-

tial conductivity occurs above $Va = 1.2$ V. Obviously, the simulated I-V characteristics under considered thermal conditions differ slightly only.

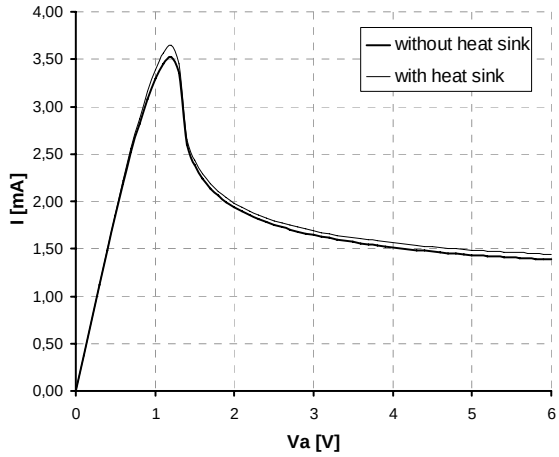

Fig. 7. I-V characteristics of Gunn diode with / without heat sink.

5.2 PIN diode

First, 1D model of Si PIN diode is analyzed assuming parameters published in [5]: free carriers concentration exceeds the value $10^{24}\,m^{-3}$ for doping concentrations $2\cdot10^{22}\,m^{-3}$ and 100 μm long low doped N-type layer (N). Fig. 8 shows the used doping profile, where the high doped P-type (P^+) layer is in the interval 0 μm to 5 μm and the high doped N-type (N^+) in the interval 105 μm to 110 μm. The transition P^+ - N is 10 μm long and transition N - N^+ is 4 μm long.

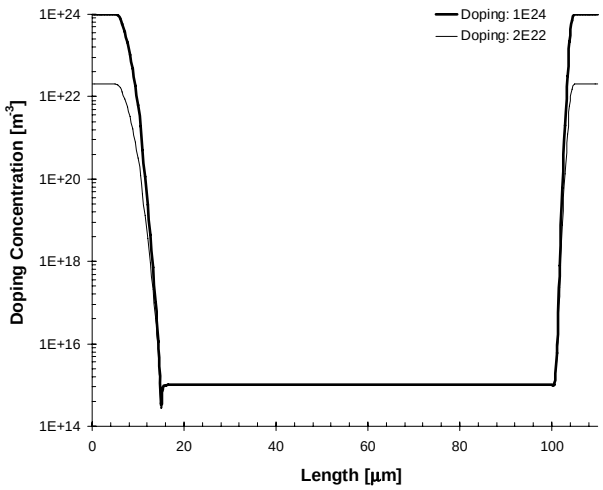

Fig. 8 The doping profiles with the concentration of dopants published in [3] (thin line) and with enhanced concentration (bold line).

The conductivity of common medium containing free carriers is given by

$$\sigma = q\sum_{i}^{M}\mu_i c_i \ , \tag{32}$$

where c is the carrier concentration and M is the number of carrier species.

The simulation was performed in voltage bias range from 0 V to 10 V. Fig. 9 shows computed distributions of the conductivity across the device at 10 V voltage bias.

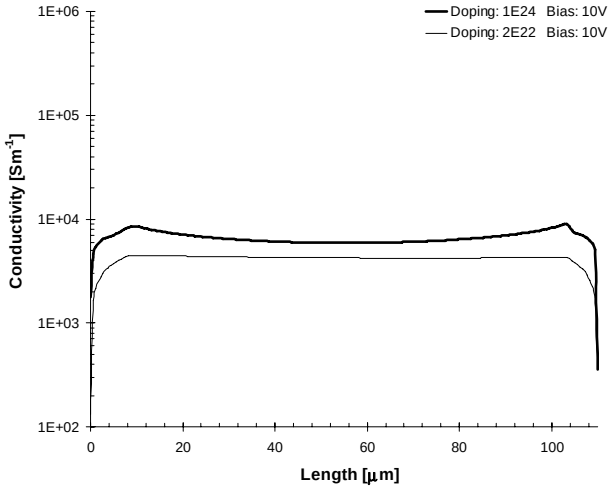

Fig. 9 The conductivity distribution across the device for concentration of dopants published in [3] (thin line) and with enhanced concentration (bold line) at 10 V bias voltage.

In order to increase the conductivity, the doping concentration was enhanced by two orders, which boosts the carrier injection effect. The bold lines in Fig. 8 and Fig. 9 present the modified doping profile and the related computed results.

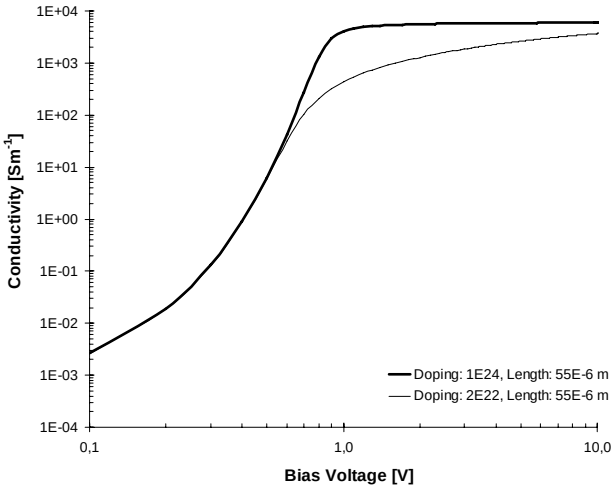

Fig. 10 The dependency of conductivity on bias voltage at the center of device (length = 55 μm) for concentration of dopants published in [3] (thin line) and with enhanced concentration (bold line).

The saturation of conductivity is fixed at the value approximately 10^4 Sm^{-1} as denotes the dependency of the conductivity on the bias voltage at the middle of the device (at length = 55 μm) for both mentioned doping concentrations presented in Fig. 10. The threshold voltage bias approximately corresponds to the diffusion potential of the diode, i.e. 0.7 – 0.8 V.

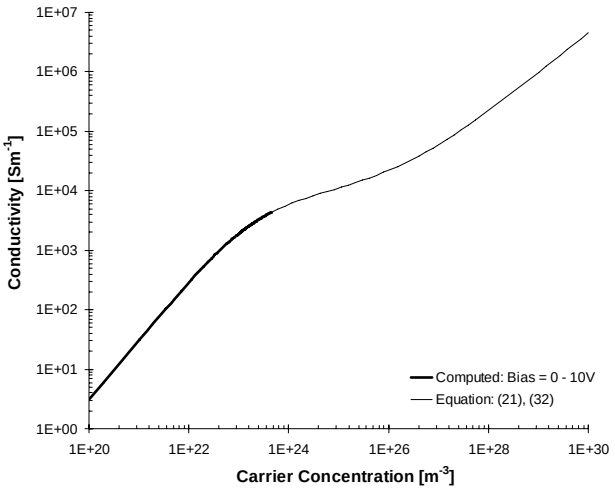

Fig. 11 The dependency of conductivity on carrier concentration in the range achieved by simulation (bold line) and given by equations (21) and (32).

The theoretical limitations are formulated by combining (20) and (21) using $\mu_{n,p}^{300}$ instead of $\mu_{n,p}^{I}$, because the ionized impurities have no effect at N layer. The resultant nonlinear progress of conductivity is shown in Fig. 11.

The conductivity distribution depicted by bold line in Fig. 9 is significantly non-uniform. This effect is related with diffusion lengths of carriers which are dependent on the diffusion constant (8) and lifetimes (11) [5].

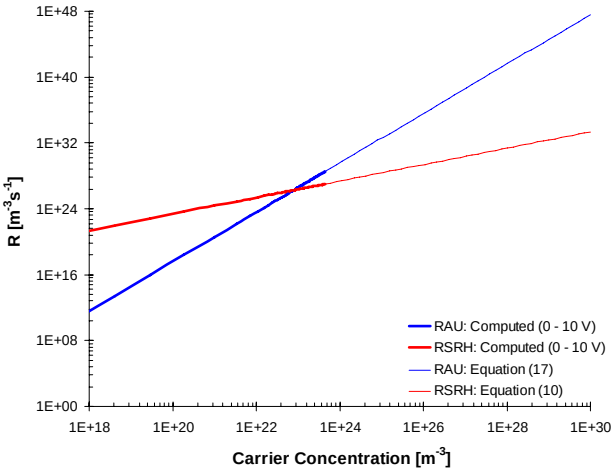

Fig. 12 The progress of the generation-recombination rates of Shockley-Read-Hall (red line) and Auger (blue line) in the carrier concentration range achieved by simulation (bold line) and given by equations (10) and (17) (thin line).

Obviously, the diffusion length is affected by the reduction of the mobility (19), and at the same time, by the generation-recombination rate because the rapid increase of the Auger generation-recombination rate (16), at carrier concentrations higher than 10^{24} m^{-3} (see Fig. 12), can be interpreted as a significant reduction of lifetimes. The computations performed with separate models of mobility and generation-recombination rates (not included in paper) declare that the Auger generation-recombination is the dominant factor. The uniform conductivity distribution can be achieved by a proper length of the N layer only in order to satisfy requirement of comparable dimensions with the carrier diffusion length [5].

6. Conclusions

The paper presents a multi-physical approach to the modeling of the Gunn diode and the PIN diode based on the electrostatic, drift-diffusion and thermal phenomena. Closed-form expressions of the important physical parameters necessary for the proper function of diodes were presented and added to basic semiconductor equations. The resultant system was solved by COMSOL Multiphysics.

In case of the Gunn diode, the solution of the electric field distribution reveals the active area of the diode, and the thermal distribution uncovers the center of the heat source under two different cooling conditions. The computed I-V characteristics prove the proper function of the model, and the thermal impact presented by the T-V characteristics is discussed.

In case of PIN diode, the conductivity increase in the intrinsic layer due to the carrier-injection effect was presented. The conductivity distribution uniformity and the dependency on the bias voltage and the free carrier concentration were discussed.

Acknowledgements

Research described in the contribution was financially supported by the Czech Grant Agency under the grants no. 102/ 07/0688 and 102/08/H018, and by the research program MSM 0021630513: Advanced Communication Systems and Technologies. The research is a part of the COST project IC0607 ASSIST.

References

[1] SELBERHERR, S. *Analysis and Simulation of Semiconductor Devices*. Hiedelberg: Springer-Verlag, 1984.

[2] *COMSOL Multiphysics Model Library*. Stockholm: COMSOL, 2006.

[3] KRAMER, K. M., HITCHON, W. N. G. *Semiconductor Devices: Simulation Approach*. Englewood Cliffs: Prentice Hall, 1997.

[4] QUAY, R. *Analysis and Simulation of High Electron Mobility Transistors* [online]. Ph.D. Thesis. Vienna: Vienna University of Technology. Available: http://www.iue.tuwien.ac.at/phd/quay/diss2.html

[5] TAYLOR, G. C., ROSEN, A., FATHY, A. E., SWAIN, P. K., PERLOW, S. M. *Surface PIN Device*. U.S. Patent US 6617670B2, 2003.

About Author...

Michal POKORNÝ was born in 1983. He is PhD student at the Brno University of Technology, Dept. of Radio Electronics. His research interests are antenna design and modeling of microwave semiconductor devices.